Scientific Journal of Silesian University of Technology. Series Transport
Zeszyty Naukowe Politechniki Śląskiej. Seria Transport

Volume 121 **2023**

p-ISSN: 0209-3324

e-ISSN: 2450-1549

DOI: https://doi.org/10.20858/sjsutst.2023.121.8

Journal homepage: http://sjsutst.polsl.pl

Article citation information:
Hong, T.D., Truong, P.T., Pham, M.Q., Tran, L.Q. Designing a compact firefighting vehicle for narrow residential areas on the base of a lawn mower. *Scientific Journal of Silesian University of Technology. Series Transport*. 2023, **121**, 107-126. ISSN: 0209-3324. DOI: https://doi.org/10.20858/sjsutst.2023.121.8.

Thong Duc HONG[1], Phat Tan TRUONG[2], Minh Quang PHAM[3], Lam Quang TRAN[4]

DESIGNING A COMPACT FIREFIGHTING VEHICLE FOR NARROW RESIDENTIAL AREAS ON THE BASE OF A LAWN MOWER

Summary. With the explosion of urbanization, more and more small residential areas with high population density, tiny houses, and narrow roads are formed. As a result, it is challenging for large fire engines to penetrate these areas in the event of a fire incident. In this paper, a compact firefighting vehicle was designed based on the SNAPPER LT140H331KV lawn mower. The vehicle is equipped with a water sprayer system and a folding frame water tank. The water sprayer system transmits power from the lawn mower transmission's power take-off shaft via the belt and chain drive, which can spray water at a height of about 13 m with a flow rate of 38 L/min. The 500-liter folding frame water tank has a rectangular shape that can be folded and dragged as a trailer. The water sprayer system and folding frame water tank not only have a simple, compact structure but also do not affect the lawn mowing function. This fire truck has a maximum speed of about 15 km/h and can move in a minimal road width of only 1.3 m, which is accommodation for residential areas within a 1÷2 km radius with narrow roads, high density of

[1] Faculty of Transportation Engineering, Ho Chi Minh City University of Technology (HCMUT), Ho Chi Minh City, Viet Nam. Email: hongducthong@hcmut.edu.vn. ORCID: https://orcid.org/0000-0002-8010-5851
[2] Faculty of Transportation Engineering, Ho Chi Minh City University of Technology (HCMUT), Ho Chi Minh City, Viet Nam. Email: phat.truong2000@hcmut.edu.vn. ORCID: https://orcid.org/0000-0001-6064-640X
[3] Faculty of Transportation Engineering, Ho Chi Minh City University of Technology (HCMUT), Ho Chi Minh City, Viet Nam. Email: phamquangminh@hcmut.edu.vn. ORCID: https://orcid.org/ 0000-0002-0407-2584
[4] Faculty of Transportation Engineering, Ho Chi Minh City University of Technology (HCMUT), Ho Chi Minh City, Viet Nam. Email: lamtq1910@hcmut.edu.vn. ORCID: https://orcid.org/0009-0008-6941-9842

population and houses in least developed and developing countries (e.g., Vietnam, Laos, Cambodia), where the normal fire engines are difficult to access in time. Besides, the vehicle can be used for watering and spraying pesticides on gardens and small premises. The study has proposed a valuable solution to take advantage of vehicle functions to improve their convenience and usefulness.

Keywords: lawn mower, firefighting vehicle, drive mechanism, water sprayer, spraying pesticides

1. INTRODUCTION

Due to the explosion of urbanization, more and more residential areas have been formed in cities recently. In residential areas, the houses and associated works are often built with a dense density to ensure that they can accommodate numerous people within the city's limited space. Consequently, ensuring fire protection on the residential campus is crucial. In developed countries, residential planning is conducted effectively. So, the infrastructure for fire safety is always guaranteed, for example, the spacious campus with large roads and various water poles so that fire trucks can quickly move in the event of a fire incident. However, residential areas in the least developed and developing countries are much less well planned due to rapid population growth and urbanization. With a huge population density, these areas have many tiny houses (with a height of about 3 or 4 floors) located close together, and the roads are very narrow and winding. When there is a fire incident, it will be challenging for bulky fire engines to penetrate and extinguish the fire promptly. Therefore, it is crucial for on-site fire vehicles with compact size, flexibility, and firefighting ability at 3÷4 floors to handle fire incidents quickly and conveniently.

On the other hand, the driver's lawn mowers from brands such as Snapper, Husqvarna, and Murray are prioritized for beautifying tourist units' lawns, such as resorts, golf courses, or universities, due to their power and convenience. However, lawn mowing only needs to be done about once per month. Outside of this working period, the lawn mower does not operate. Hence, improving the lawn mower into a multi-function vehicle will increase the vehicle's value at an affordable investment cost [4-7].

The lawn mowers are compact, flexible in turning, and have high engine power. Therefore, renovating the lawn mower into a compact firefighting vehicle has a significant impact on increasing its adequate use time and quickly extinguishing an unexpected residential fire. With an existing engine and chassis, the additional investment cost will be much lower than an entirely new one.

In this paper, the authors design a compact firefighting vehicle based on the Snapper LT14H331KV lawn mower for use on the residential campus. A water sprayer system is installed on the lawn mower's rear; the water sprayer extracts power from the lawn mower transmission's power take-off shaft by the chain and belt drive mechanisms. The water sprayer system is calculated to spray water to the height of the 3rd floor. In addition, a folding frame tank with folding ability is equipped to serve water when fighting a fire. With the water sprayer system and folding frame tank equipped, the vehicle can still move in residential areas with a minimum road width of around 1.3 m and a maximum speed of around 15 km/h, which can be applied in several residential areas within a radius of 1÷2 km. Moreover, the vehicle can be utilized for pesticide application and watering plants on the premises.

2. GENERAL LAYOUT DESIGN

The structure of the SNAPPER LT140H331KV lawn mower, shown in Fig. 1, has an overall dimension of 1220×880×770 mm in L×W×H. The engine is a Kohler Command CV14 with maximum power and torque of 14 HP/3600 rpm and 28.9 Nm/2500 rpm, respectively [8]. The maximum speed of the vehicle is around 15 km/h. The lawn mower is equipped with two cutting blades under the vehicle, which is driven by a belt drive. The vehicle powertrain system includes an engine, a belt drive with a 1:1 gear ratio, and a BDU-10S hydrostatic transmission. In addition to driving the two rear wheels, the transmission has a power take-off shaft that can extract power for other functions.

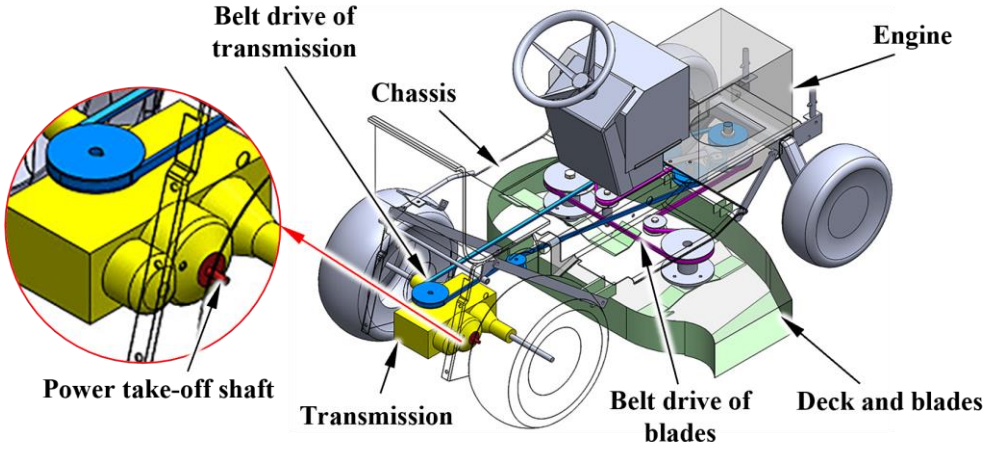

Fig. 1. Structure of the original lawn mower

The structure of the compact firefighting vehicle is illustrated in Fig. 2. Based on the structure of the original lawn mower, the authors arranged a water sprayer system and a folding frame water tank with a compact, lightweight structure and ensured the vehicle's performance. The water sprayer system is located at the lawn mower's rear and is powered by the transmission, including the water sprayer, water sprayer drive mechanisms, and water sprayer disengage mechanism. The water sprayer is mounted on a base that is tightly fitted to the chassis. The water sprayer drive, which transmits the power from the power take-off shaft to the water sprayer, consists of a chain drive and a belt drive, linked by an intermediate shaft and feather keys. The water sprayer disengagement mechanism is installed on the belt drive to disengage and engage the water sprayer drive rapidly and conveniently. The water sprayer disengagement mechanism switches the water sprayer on or off and acts as a belt tensioner. The workings of this mechanism are presented in Fig. 3. When the control arm is pulled up, the roller pushes the belt and creates the belt tension force, leading to the belt drive being activated. In contrast, when the control arm is pulled down, the roller is not in contact with the belt, leading to the belt drive being deactivated. When the control arm is pulled up, the roller pushes the belt and creates the belt tension force, activating the belt drive. In contrast, when the control arm is pulled down, the roller is not in contact with the belt, deactivating the belt drive. The detailed calculation of the water sprayer system is presented in Sections 3 and 4.

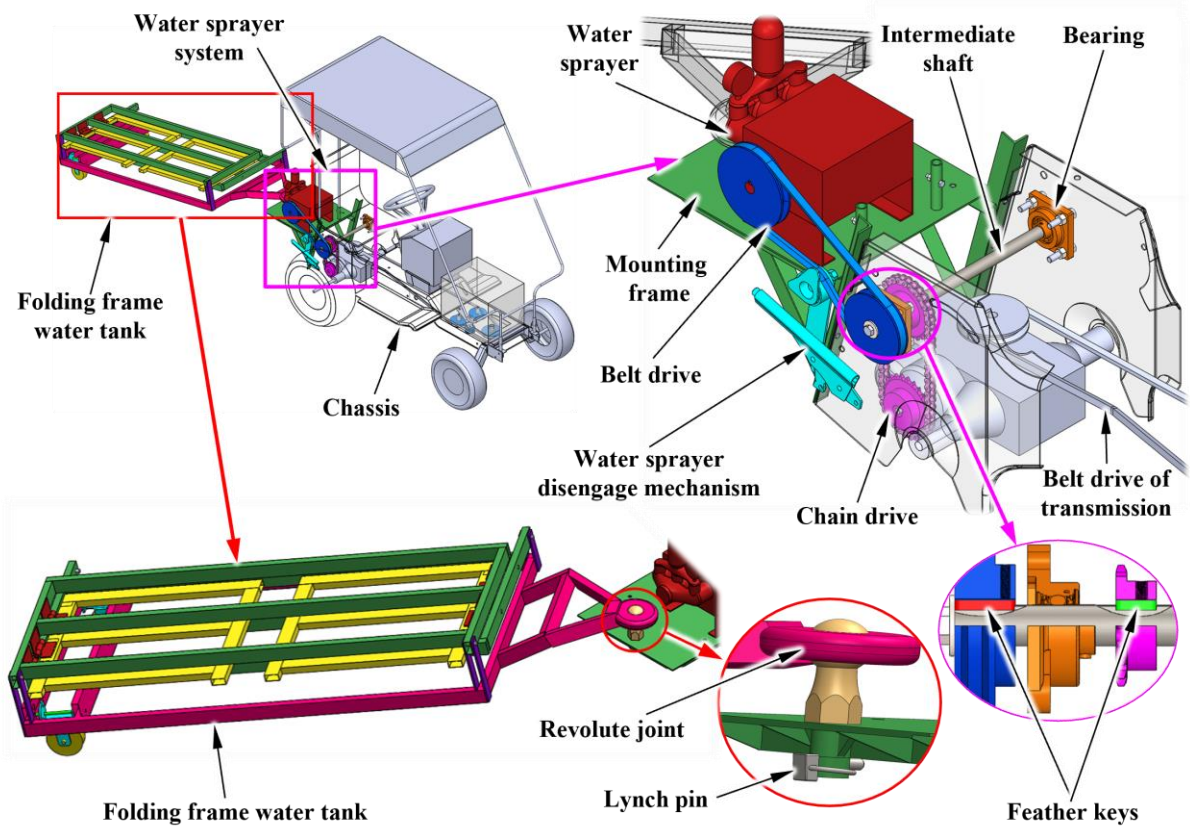

Fig. 2. Construction of the compact firefighting vehicle

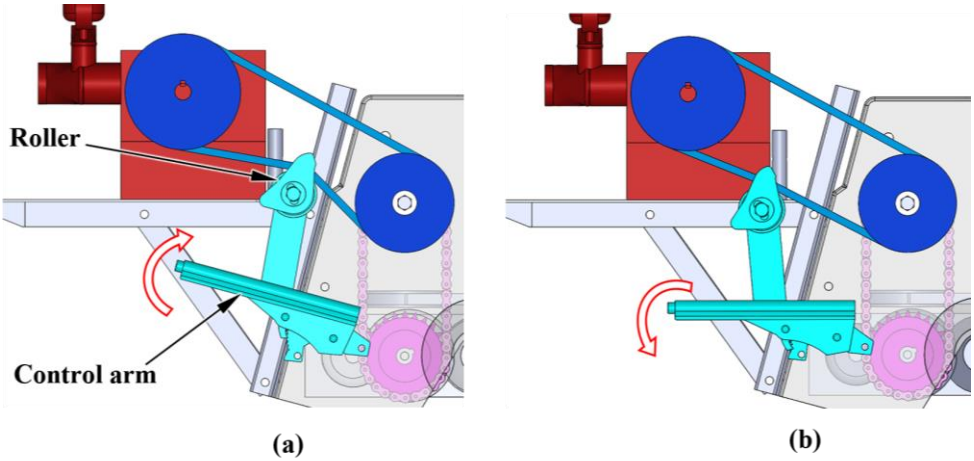

Fig. 3. Water sprayer disengagement mechanism (a) Engage, (b) Disengage

The folding-frame tank is assembled from steel bars and comes with an awning to hold the water. In the moving process, the frame and awning are folded and dragged behind like a trailer via the revolute joint and lynch pin; when reaching the fire point, the frame is quickly disassembled from the vehicle and placed on the ground by releasing the lynch pin, then assembled into a box shape, and an awning is spread inside to contain water. With the aim of fighting fires in residential areas, the size of the folding frame tank is designed to ensure that it

can hold 500 liters of water while keeping the required space for turning minimal. The water tank has overall dimensions in L×W×H of 1700×660×330 mm in the folded state and 1700×660×660 mm in the working state. The steering kinematic diagram of the fire truck is shown in Fig. 4. Fig. 4a and Fig. 4b present the cases of vehicle steering with a minimum turning radius and minimum required space of 1250 mm and 1300 mm, respectively. The detailed structure of the folding frame water tank is illustrated in Section 5.1.

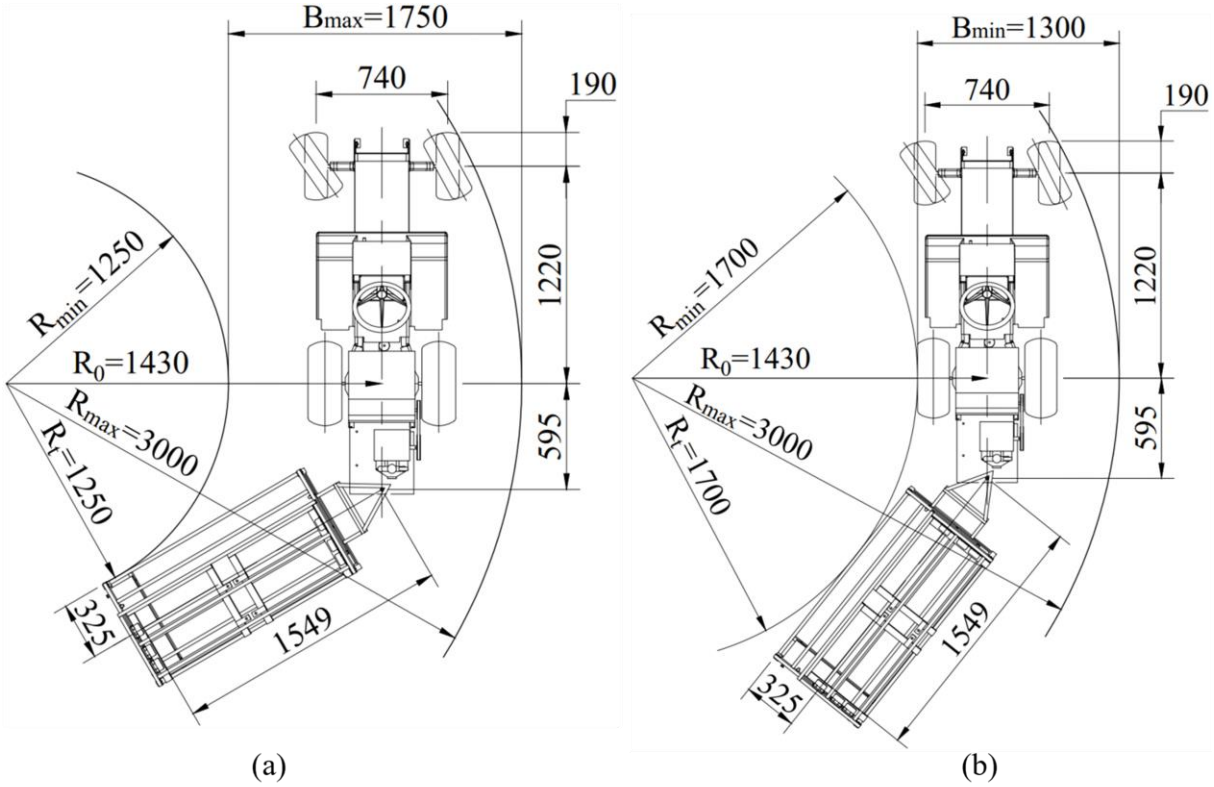

Fig. 4. Kinematic steering condition of compact firefighting vehicle (a) Minimum turning radius R_{min}, (b) Minimum required space B_{min}

3. CALCULATING NOZZLE AND DETERMINING THE ACTUAL CHARACTERISTICS OF A WATER SPRAYER SYSTEM

The SCN-30 power sprayer was selected to take responsibility for spraying water. It has an overall dimension of 390×320×300 mm in L×W×H and a weight of 12 kg, which makes it suitable for installation on lawnmowers. This water sprayer has a maximum required power of 2.2 kW, maximum pressure of 40 kg/cm^2, maximum capacity of 42 L/min, and an operation speed range of 300 to 1000 rpm [9]. The water sprayer has a suction hole and two outlet holes with diameters of 20, 8, and 21 mm, respectively. With the drive system as presented in Section 2 (see Fig. 2), the required engine power is determined by equation (1) [10]. The required power is much smaller than the engine power, so the selected water sprayer is suitable.

$$P_{e\_r} = P_p / \eta_b \eta_g \eta_{ch} \eta_b = 2.56 \text{ (kW)} \quad (1)$$

Where η_b = 0.95, η_g = 0.99 and η_{ch} = 0.96 are the efficiency of belt drive, gear drive and chain drive, respectively. P_{e_r} and P_p = 2.2 kW are the required engine power and the water sprayer's maximum power required, respectively.

The outlet diameter of the nozzle will be calculated to be able to spray water at a height of about 15m (corresponding to the height of the normal building's 3rd floor). Then, the actual characteristics of the water sprayer system are determined by experiments to ensure real working efficiency.

3.1. Calculating the nozzle

It must be determined whether the water jet's velocity is necessary before determining the nozzle's dimension. For firefighting vehicles, the water jet always needs to reach the required height and be able to travel the farthest. With 15 meters of required water jet height, the water jet's velocity at the nozzle is determined by the following formula [11]:

$$v_o = \sqrt{(H-h)2g/\sin(\alpha)^2} = 18{,}8 \text{ (m/s)} \quad (2)$$

Where v_o is the water jet's velocity at the nozzle. g is gravity's acceleration. H = 15 m, h = 1.5 m, α = 60° are the maximum height, initial height, and initial angle of the water jet, respectively.

The nozzle diameter is determined as below [11]:

$$d = \sqrt{\frac{Q}{v_o \pi}} = 0{,}00688 \text{ (m)} \quad (3)$$

Where d is diameter of nozzle. Q = 42 L/min = 0.0007 m^3/s is the maximum flow rate of the water sprayer.

The dimensions and shape of the nozzle are shown in Fig. 5. The nozzle has a converging shape to minimize the loss of the sprayed water.

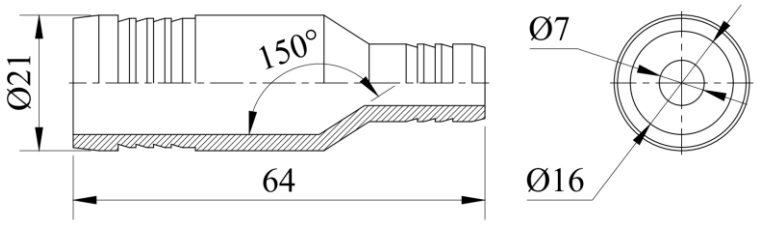

Fig. 5. Nozzle dimensions

3.2. The actual characteristics of the water sprayer system

Fig. 6 shows the water flow rate and pressure characteristics of the SCN 30 water sprayer system, which were determined by an experiment in the water sprayer speed range of 700 ÷ 1100 rpm. The experiment system includes the SCN 30 water sprayer, suction pipe with 2000 mm long and 20 mm diameter, outlet pipe with 5000 mm long and 21 mm diameter, and a nozzle with a diameter of 7 mm. The results show that, with a water sprayer speed of 1000 rpm,

the water sprayer can generate a water flow rate of about 38 L/m with a pressure of 5.5 kg/cm^2. The generated water jet reaches a height of about 13 m, which corresponds to the height of the 3rd floor of the building at Ho Chi Minh City University of Technology, see Fig. 7.

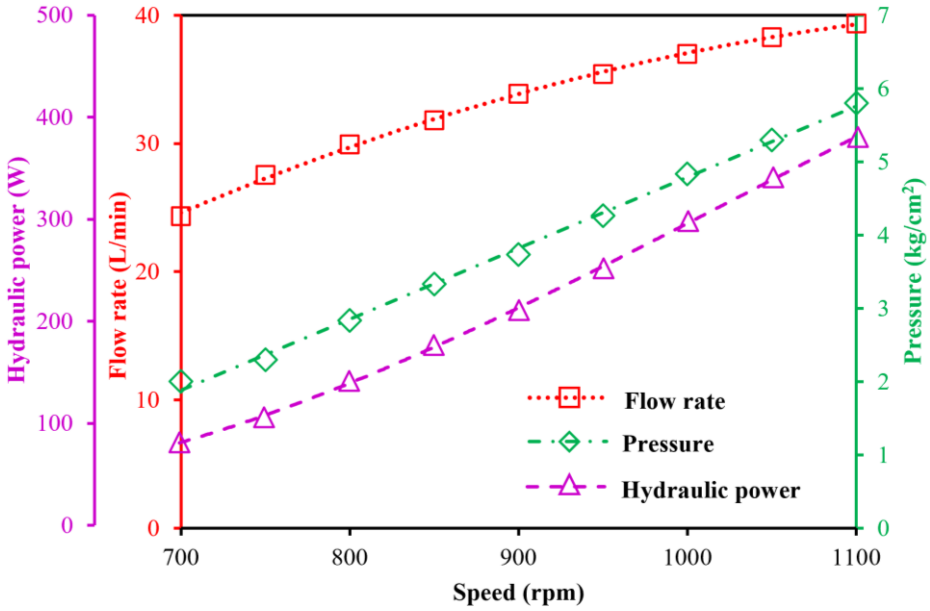

Fig. 6. The actual water sprayer system characteristics curve

Fig. 6 shows the water flow rate and pressure characteristics of the SCN 30 water sprayer system, which were determined by an experiment in the water sprayer speed range of 700 ÷ 1100 rpm. The experiment system includes the SCN 30 water sprayer, suction pipe with 2000 mm long and 20 mm diameter, outlet pipe with 5000 mm long and 21 mm diameter, and a nozzle with a diameter of 7 mm. The results show that, with a water sprayer speed of 1000 rpm, the water sprayer can generate a water flow rate of about 38 L/m with a pressure of 5.5 kg/cm^2. The generated water jet reaches a height of about 13 m, which corresponds to the height of the 3rd floor of the building at Ho Chi Minh City University of Technology, see Fig. 7.

4. CALCULATING THE WATER SPRAYER DRIVE

The water sprayer drive cluster includes the chain, belt drive mechanism, and intermediate shaft (see Fig. 2). In which the intermediate shaft contains two bearings and two feather keys. Hence, all these components are considered in this section.

4.1. Speed ratio distribution

The Kohler Command CV14 engine has an idle speed of about 1400 rpm. Meanwhile, the water sprayer's working speed range is 1000 rpm. Hence, an overall transmission ratio of 1.4 is chosen. To facilitate the structural design and ensure the simplification of the drive mechanism, the chain drive and belt drive speed ratios are estimated at u_{ch} = 1 and u_b = 1.4, respectively. With the drives' efficiency determined in Section 3 and the transmission ratios determined above, the technical characteristics of the water sprayer drive are summarized in Tab. 1.

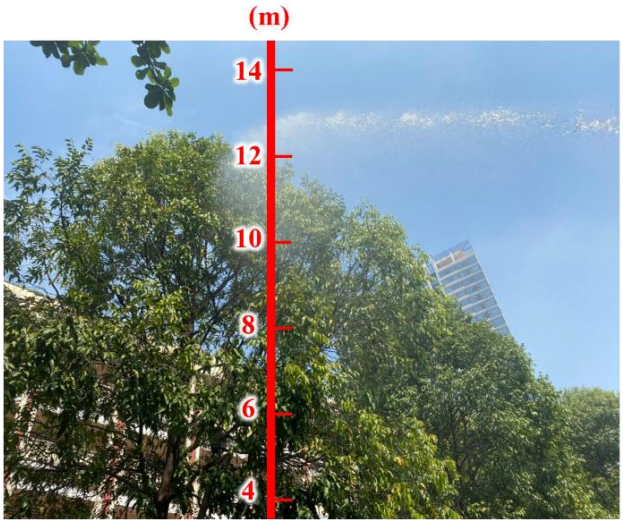

Fig. 7. Realistic picture of water jet

Tab. 1

Technical characteristics of the powertrain system

Parameters	Engine	Chain drive	Belt drive
Power (kW)	P_e = 2.6	P_{ch} = 2.45	P_b = 2.3
Transmission ratio	u_{ch} = 1	u_b =1.4	
Rotational speed (rpm)	n_e = 1400	n_{ch} = 1400	n_b = 1000

4.2. Calculating the chain drive

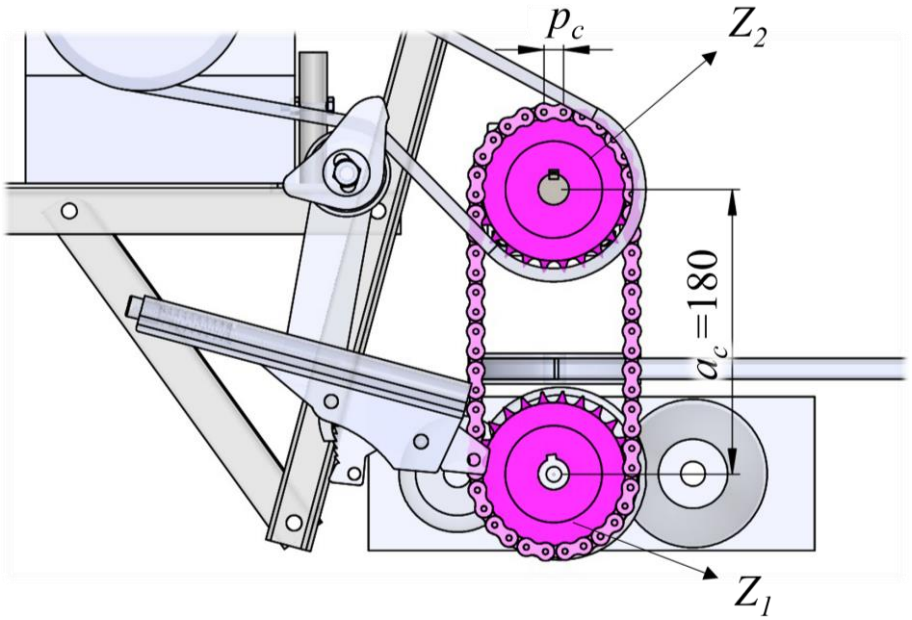

Fig. 8 Chain drive arrangement

The arrangement of the chain drive is shown in Fig. 8. According to the general layout design, the chain drive is arranged vertically, including the initial center distance a_c = 180 mm, driving sprocket Z_1, driven sprocket Z_2, and chain pitch p_c.

The chain drive mechanism must be able to transmit 2.6 kW power from the Korman engine at a rotational speed of 1400 rpm to drive the water sprayer. This drive mechanism can be considered a smooth transmission with no impact. Hence, the service factor $F_{C\_1} = 1$ is selected [10]. Assuming the multiple strand factor $F_{C\_2} = 1$, the required power rating is obtained from the equation below [10]:

$$P_{R\_ch} = P_e \frac{F_{C\_1}}{F_{C\_2}} = 2.6 \times \frac{1.2}{1} = 3.12 \text{ (kW)} \tag{4}$$

Where P_e = 2.6 kW is engine power.

Searching the design guideline for standard roller chains [10] for a combination of 1400 rpm and 3.12 kW provides an ANSI No. 35 chain with a single strand that can be used for this application. Besides, due to the chain drive's transmission ratio of 1, 18 teeth for both sprockets are also selected.

The number of links X is estimated by equation (5). Hence, the number of links selected is 56.

$$X = \frac{L_c}{p_c} = \frac{2a_c}{p_c} + \frac{Z_1 + Z_2}{2} + \frac{\left(Z_2 - Z_1\right)^2}{4\pi^2 \left(\frac{a_c}{p_c}\right)} = 55.80 \text{ (links)} \tag{5}$$

Where L_c is chain length (mm), a_c is the center distance (mm), p_c = 9.525 mm, $Z_1 = Z_2 = 18$ teeth are the chain pitch and the number of teeth of the driving and driven sprocket, respectively.

The chain length is calculated by the following formula [10]:

$$L_c = X p_c = 531.45 \text{ (mm)} \tag{6}$$

Hence, an actual center distance is determined based on the following formula [10]:

$$a_c = p_c \left[\frac{1}{4}\left(\frac{L_c}{p_c} - \frac{Z_1 + Z_2}{2} \right) + \sqrt{\left[\frac{1}{4}\left(\frac{L_c}{p_c} - \frac{Z_1 + Z_2}{2} \right) \right]^2 - \frac{\left(\frac{Z_2 - Z_1}{2\pi} \right)^2}{2}} \right] = 180.98 \text{ (mm)} \tag{7}$$

It should be noted that the center distance needs to be decreased by 1% to allow for a bit of slack, resulting in an actual center distance of within 179 mm.

Chain velocity is obtained by the following formula [10]:

$$v_{ch} = \frac{Z_1 p_c n_e}{60000} = 4.00 \text{ (m/s)} \tag{8}$$

Where v_{ch} is the chain velocity (m/s), the chain pitch p_c = 9.525 mm and n_e = 1400 rpm is the engine speed.

The tangential force or shaft load on the sprocket is calculated below [10]:

$$F_{r\_ch} = \frac{1000.P_e}{v_{ch}} = 612.5 \text{ (N)} \quad (9)$$

Where F_{r_ch} is the tangential force or shaft load on the sprocket, P_e = 2.6 kW is the engine power.

The final parameters of the chain drive are summarized in Tab. 2 and Fig. 9 as follows.

Tab. 2

Parameters of the chain drive

Parameters	Symbol	Value	Unit
Type	-	40B	-
Chain pitch	p_c	9.525	mm
Sprocket teeth	Z_1, Z_2	18	teeth
Number of pitches	X	56	pitches
Chain length	L_c	531.45	mm
Center distance	a_c	180.98	mm
Number of strands	-	1	strand

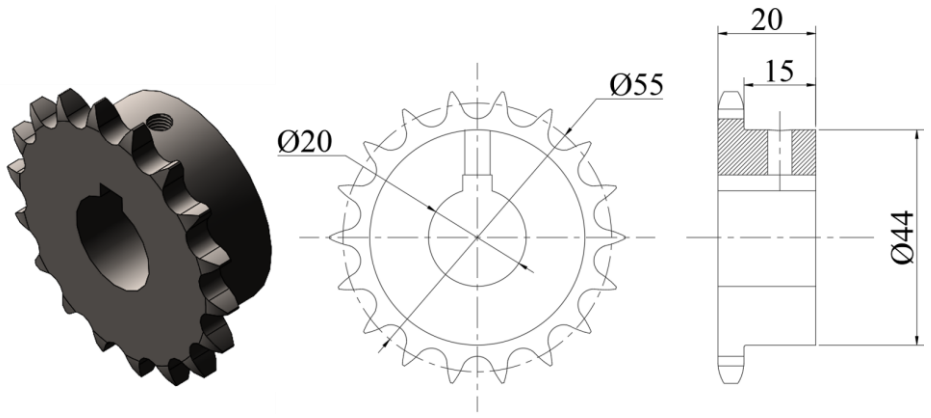

Fig. 9. Geometric parameters of chain sprockets

4.3. Calculating the belt drive

The arrangement of the belt drive is shown in Fig. 10. According to the general layout design, the initial parameters of the belt drive are selected with the center distance a_b, and the inclined angle α being 300 mm, and 26 degrees, respectively. The belt drive includes a driving pulley with diameter d, a driven pulley with diameter D and V-belt with thickness t and width b.

With the power and rotational speed as shown in Tab.1 and the operating conditions are mentioned in section 4.2, the correction factor of belt drive F_{B_1} is selected at 1.1 [10]. The belt drive's design power is determined by the following relationship [10]:

$$\text{Design power} = F_{B\_1} \times P_{ch} = 2.69 \text{ (kW)} \quad (10)$$

Where F_{B_1} = 1.1 is the correction factor of the belt drive.

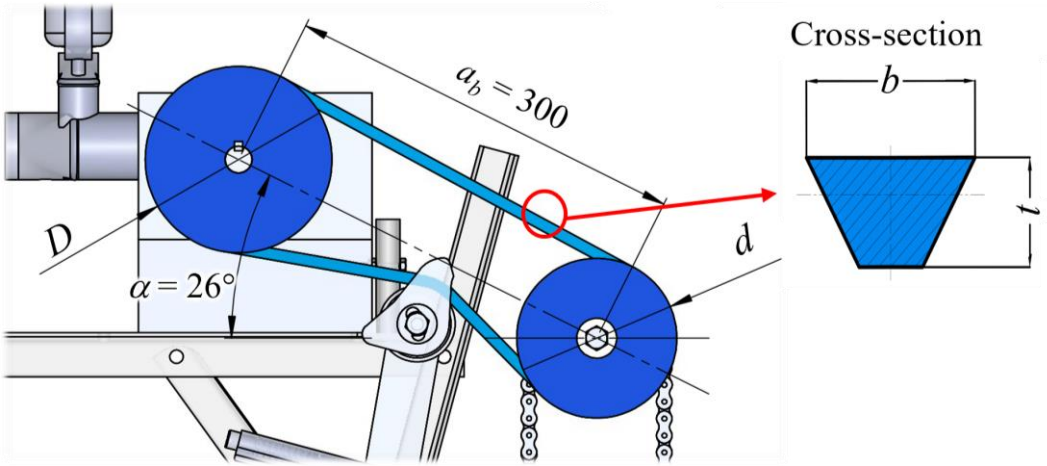

Fig. 10. Arrangement of belt drive

With the driving pulley's rotational speed of 1400 rpm and the design power of the belt drive determined above, type A of the V-belt is preliminary selected [10]. Hence, the pitch diameter of the driving pulley is 125 mm. The pitch diameter of the bigger pulley is calculated below [10]:

$$D = d\left[\frac{\text{Speed of smaller pulley}}{\text{Speed of bigger pulley}}\right] = d\left[\frac{\text{Input speed}}{\text{Output speed}}\right] = d\frac{n_{ch}}{n_b} = 175 \text{ (mm)} \quad (11)$$

Where d = 125 mm and D are the pitch diameters of smaller and bigger pulleys, respectively, n_{ch} = 1400 rpm and n_b = 1000 rpm are the input speed and output speed of the belt drive, respectively.

Due to the fact that 175 mm is a non-standard value for the type A pulley diameter, the nearest diameter of the bigger pulley value D is selected at 180 mm [10]. Hence, the transmission ratio of the belt drive is recalculated by equation (12) [10]. The difference between the actual and estimated transmission ratio is about 3%, which can be ignored.

$$u_b = \frac{D}{d} = 1.44 \quad (12)$$

The Ppitch length of the belt L_b is determined as follows [10]:

$$L_b = 2a_b + \frac{\pi(D+d)}{2} + \frac{(D-d)^2}{4a_b} = 1081.61 \text{ (mm)} \quad (13)$$

Where L_b is the pitch length of the belt (mm), a_b = 300 mm is the center distance of the belt drive.

From reference [10], the recommended pitch length for type A belt is between 990 and 1100 mm. As a result, the belt's pitch length is chosen at 1100 mm. Substituting the pitch length above into equation (13). Hence, the correct center distance a_b is 309 mm.

With type A and a 1100 mm belt length, the correction factor for belt length F_{B_2} is 0.90 [10]. The smaller pulley's arc of contact is estimated as follows [10]:

$$\alpha_s = 180 - 2\sin^{-1}\left(\frac{D-d}{2a_b}\right) = 169.79^\circ \geq 120^\circ \quad (14)$$

Where α_s is the smaller pulley's arc of contact.

Hence, the correction factor for the arc of contact F_{B_3} is selected at 0.97 [10]. From reference [10], the power rating of the single V-Belt P_r is 2.32 kW due to the driving pulley having a rotational speed of 1400 rpm, the smaller pulley d is 125 mm, and the speed ratio is 1.44. The number of belts required for the transmission is calculated below [10]:

$$\text{Number of belts} = \frac{P_{ch} \times F_{B\_1}}{P_r \times F_{B\_2} \times F_{B\_3}} = 1.33 \text{ or } 1 \text{ (belt)} \quad (15)$$

Where P_r = 2.32 kW, F_{b_2} = 0.90, and F_{b_3} = 0.97 are the V-Belt power rating, the belt length correction factor, and the correction factor for arc of contact, respectively.

The average velocity of the belt drive is calculated as follows [10]:

$$v = \frac{\pi d n_{ch}}{6 \times 10^4} = 9.16 \text{ (m/s)} \quad (16)$$

Where n_{ch} = 1400 rpm is the rotational speed of the driving pulley.

The maximum belt tension can be estimated by the following formula [10]:

$$P_{\max} = bt\sigma = 182 \text{ (N)} \quad (17)$$

Where b = 13 mm, t = 8 mm are the width and thickness of the belt [12], σ = 1.75 N/mm^2 is the maximum permissible tensile stress for the belt material [13].

The shaft load created by the belt drive is determined as follows:

$$F_{r\_b} \approx 2P_{\max} \sin\frac{\alpha_s}{2} \approx 362.56 \text{ (N)} \quad (18)$$

Where F_{r_b} is the belt drive's shaft load, P_{max} = 182 N is the maximum belt tension.

Hence, the horizontal and vertical forces created by the belt drive are calculated as below:

$$F_{C\_x} = F_{r\_b} \times \sin\alpha = 158.94 \text{ (N)} \quad (19)$$

$$F_{C\_y} = F_{r\_b} \times \cos\alpha = 325.87 \text{ (N)} \quad (20)$$

Where F_{C_x} and F_{C_y} are the horizontal and vertical forces created by the belt drive, respectively. α = 26 degrees is the inclined angle of the belt drive's arrangement.

The final parameters of the belt drive are summarized in Tab. 3 as follows.

Tab. 3

Parameters of the belt drive

Parameters	**Symbol**	**Value**	**Unit**
Type	-	A	-
Diameter of the driving pulley	d	125	mm
Diameter of the driven pulley	D	180	mm

Belt length	L_b	1100	mm
Center distance	a_b	309	mm
Number of belts	-	1	belt

4.4. Calculating the intermediate shaft strength

The detailed structure of the intermediate shaft is shown in Fig. 11. The intermediate shaft supports transmission elements and connects the inputs and outputs of the compact firefighting vehicle's drivetrain. Hence, it is subjected to the combinations of bending moment and torsional moment, which are created by the chain drive and belt drive. Besides, it is designed with a diameter of 20 mm, which is equal to the available hub diameter of the chain sprocket and pulley, a length of 400 mm, and is made of AISI 1045 steel material. The factor of safety *(fs)* for strength calculation is chosen at 3.

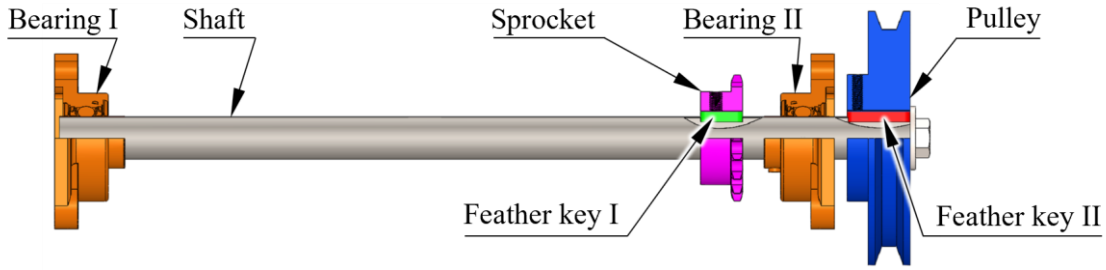

Fig. 11. Structure of intermediate shaft

In sections 4.2 and 4.3, the chain drive and belt drive's shaft loads have been determined, which include $F_{r\_ch} = F_{By} = 612.5$ N as the chain drive's shaft load, belt drive's shaft load is decomposed into F_{Cx} and F_{Cy} with values 158.94 N and 325.87 N respectively. The torque exerted on the shaft is calculated by the following formula [10]:

$$T = \frac{9550 \times P_{ch}}{n_{ch}} = 16.71 \text{ (Nm)} \quad (21)$$

Where T is the torque exerted on shaft (Nm), $P_{ch} = 2.45$ kW is the power created on the shaft by chain drive.

In this study, Solidworks Simulation is used to calculate the strength of the intermediate shaft. Fig. 12 presents the forces and torque acting on the shaft and imported into this software.

The reaction forces on the intermediate shaft at the bearing locations (sections A and C) are shown in Fig. 13. It can be seen that the bearing in section C is subjected to a much larger load than the bearing in section A due to the location of the applied forces near this bearing.

The stress distribution of the intermediate shaft is shown in Fig. 14. The results indicate that the position subject to the maximum stress occurs at the sprocket's keyseat and has the value $\sigma_{max} = 34.60$ N/mm^2 < $[\sigma] = 136.67$ N/mm^2 (corresponding with AISI 1045 Steel, and the factor of safety (*fs*) is 3) [14]. Hence, the intermediate shaft ensures the strength, rigidity, and stability of the drive system.

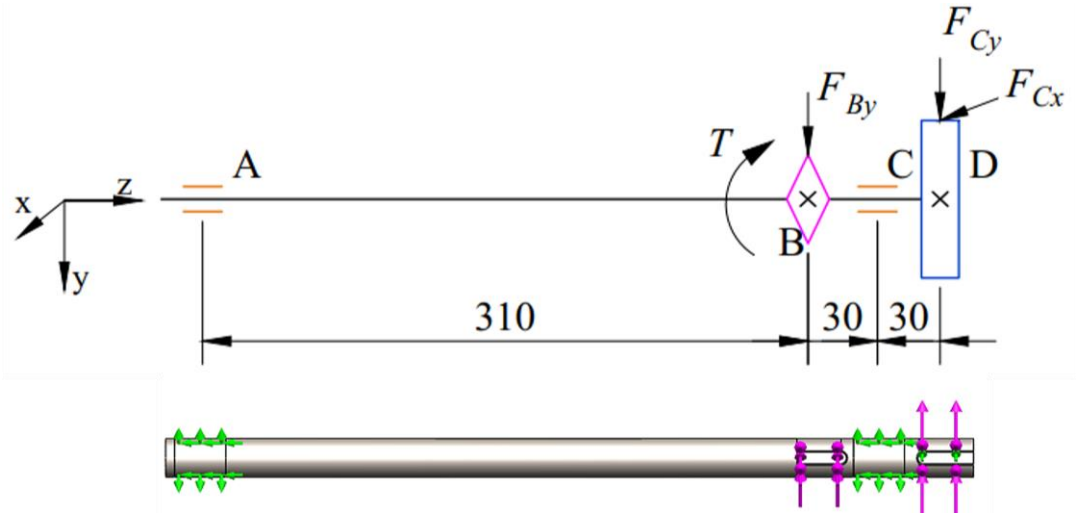

Fig. 12. Forces and torque applied to the intermediate shaft

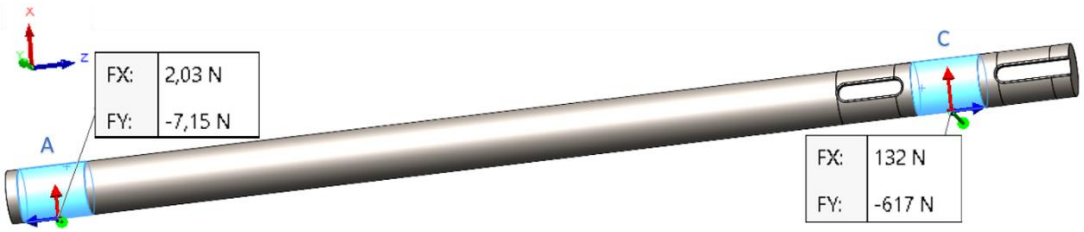

Fig. 13. Reaction forces on sections A and C of the intermediate shaft

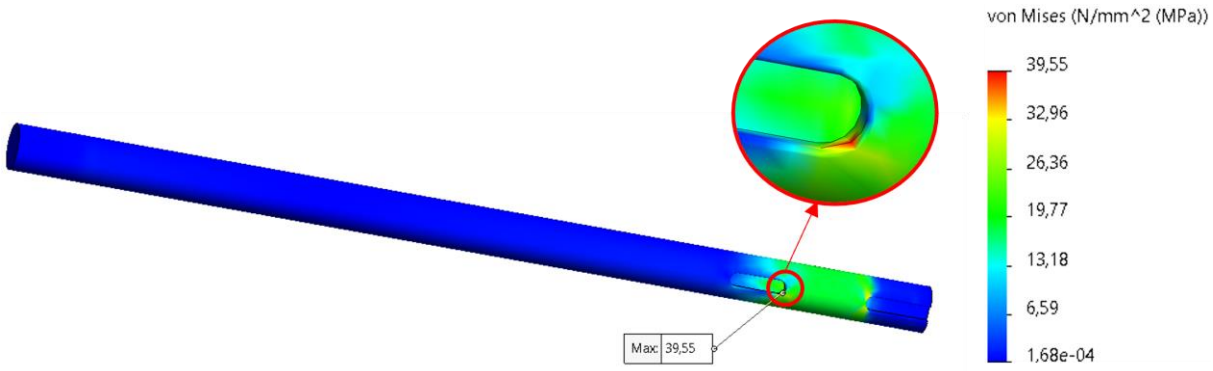

Fig. 14. Stress distribution on the intermediate shaft

4.5. Calculating the feather keys

Two feather keys are located in the intermediate shaft, which is shown in Fig. 11. These keys have two basic functions, (1) to transmit the torque from the shaft to the hub of the chain sprocket and pulley, (2) and to prevent the relative motion between the shaft and the mating elements. Hence, these keys withstand shear and compressive stresses resulting from the transmission of torque.

The key is made of AISI 1045 steel, and the factor of safety *(fs)* for calculation is chosen at 3. In this calculation, the compressive yield strength is supposed to be equivalent to the tensile

yield strength, which is $S_{yc} = S_{yt} = 410$ N/mm^2 [14]. Permissible compressive and shear stresses are estimated as follows [10]:

$$\sigma_c = \frac{S_{yc}}{(fs)} = \frac{S_{yt}}{(fs)} = 136.67 \text{ (N/mm}^2\text{)} \tag{22}$$

Where σ_c is the permissible compressive stress (N/mm^2), *(fs)* = 3 is the factor of safety. S_{yc}, S_{yt} are the yield strengths in compression and tension, respectively.

According to the maximum shear stress theory of failure, the shear yield strength is half of the tensile yield strength [10]. Hence, the permissible shear stress is determined as follows [10]:

$$\tau = \frac{S_{sy}}{(fs)} = \frac{0.5S_{yt}}{(fs)} = 68.33 \text{ (N/mm}^2\text{)} \tag{23}$$

Where τ, S_{sy} are the permissible shear stress and the yield strength in shear (N/mm^2), respectively.

The shaft transmits 16.71 Nm of torque and has a diameter of 20 mm. Hence, the industrial standard is to utilize a feather key with sides equal to one-quarter of the shaft diameter. [10]. Therefore,

$$b = h = \frac{d}{4} = \frac{20}{4} = 5 \text{ mm} \tag{24}$$

Where *b*, *h* are the feather key's width and height of (mm), respectively. *d* = 20 mm is the diameter of the intermediate shaft.

The length of the feather key is calculated below [10]:

$$l = \frac{2T}{\tau db} = 4.89 \text{ (mm)} \tag{25}$$

Where *l* is the feather key length (mm), *T* = 16.71 Nm is the torque exerted on the shaft.

After calculating the length of the feather key, according to [15], the dimensions of the key are 5×5×8 mm. However, the feather key dimensions are selected at 5×5×20 mm and 5×5×25 mm to with the overall length of the chain sprocket and the belt pulley, respectively.

4.6. Calculating the bearing

Two bearings are attached to the vehicle chassis, which supports the shaft and holds it in the correct position (See Figs. 2 and 11). So, the bearings take up the forces that act on the shaft. According to the reaction forces acting on the shaft, as shown in Fig. 13, section C is the critical section of the intermediate shaft. Hence, the radial force on the bearing is calculated in section C [10]:

$$F_{r\_C} = \sqrt{R_{Cx}^2 + R_{Cy}^2} = 630.96 \text{ (N)} \tag{26}$$

Where F_{r_C} is the radial force on the bearing at section C. R_{Cx} = 132 N, R_{Cy} = 617 N are the reaction forces on the horizontal and vertical planes, respectively.

The equivalent dynamic load is determined using the equation below [10]:

$$P = XVF_{r\_C} + YF_a = 630.96 \text{ (N)} \tag{27}$$

Where X, Y are the factors of radial and axial loading, respectively, due to the bearing just withstanding radial loads, hence, $X = 1$, $Y = 1$ [10], $V = 1$ is the factor of the rotating ring, due to the inner race rotating [10] and $F_a = 0$ is an axial load.

The bearing life is calculated as follows [10]:

$$L_{10} = \frac{60 n_{ch} L_{10h}}{10^6} = 640 \text{ (million revolutions)} \quad (28)$$

Where L_{10} is the bearing life (million revolutions), $L_{10h} = 8000$ hours is the rated bearing life.

The dynamic load capacity is determined as below [10]:

$$C = P\left(L_{10}\right)^{1/3} = 5437.45 \text{ (N)} \quad (29)$$

Where C is the dynamic load capacity (N), $P = 630.96$ N is the equivalent dynamic load.

Hence, the SKF UCF204 Square Flanged Ball Bearing is used for the system with the following technical data [16]: a limiting speed at 6500 rpm, basic dynamic load rating C and basic static load rating C_0 are 12.7 kN and 6.7 kN correspondingly.

5. FOLDING FRAME WATER TANK

5.1. Structure of a folding frame water tank

Fig. 15 reveals the structure as well as the process from the transport state into the working state of the folding frame water tank. The frame is made of SS400 steel with a cross-section of 40×20×1.2 mm, including a frame bottom, two large sidewalls with horizontal beams connected to the bottom of the frame by hinge joints, two small sidewalls attached to a large sidewall also by hinge joints, two wheels, and a revolute joint. In the transport state, the sidewall is folded, and the frame has an overall dimension of 1700×660×330 mm. The frame connects to the vehicle chassis and is dragged like a trailer by the revolute joint and lynch pin. When the vehicle reaches the emergency location, the folding frame water tank is quickly released via lynch pin. Two wheels are folded down and fixed by the locating pin, which places the frame on the ground. Then, the large sidewalls are opened. Finally, two smaller sidewalls are opened via hinge joints and linked to the other large sidewalls by buckles. By taking advantage of the ground, the bottom of the folding-frame water tank does not have beams. Then, an awning is spread inside to contain the water. In its working state, the folding frame water tank has an overall dimension of 1700×660×660 mm. Furthermore, the frame is only about 30 kg, which is enough to bring by hand if necessary.

5.2. Calculating folding frame water tank strength

The folding frame water tank's strength is simulated by Solidworks Simulation to verify the load capacity when it is containing water. When operating, the folding frame tank contains 500 liters of water with a weight of about 500 kg, so the walls of the frame are under pressure that gradually increases from the top to the bottom of the frame according to the law of hydrostatic pressure. The frame's load distribution diagram and meshing model are shown in Fig. 16. The element type is the shell element. Curvature – base mesh type is selected with a maximum element size of 18 mm.

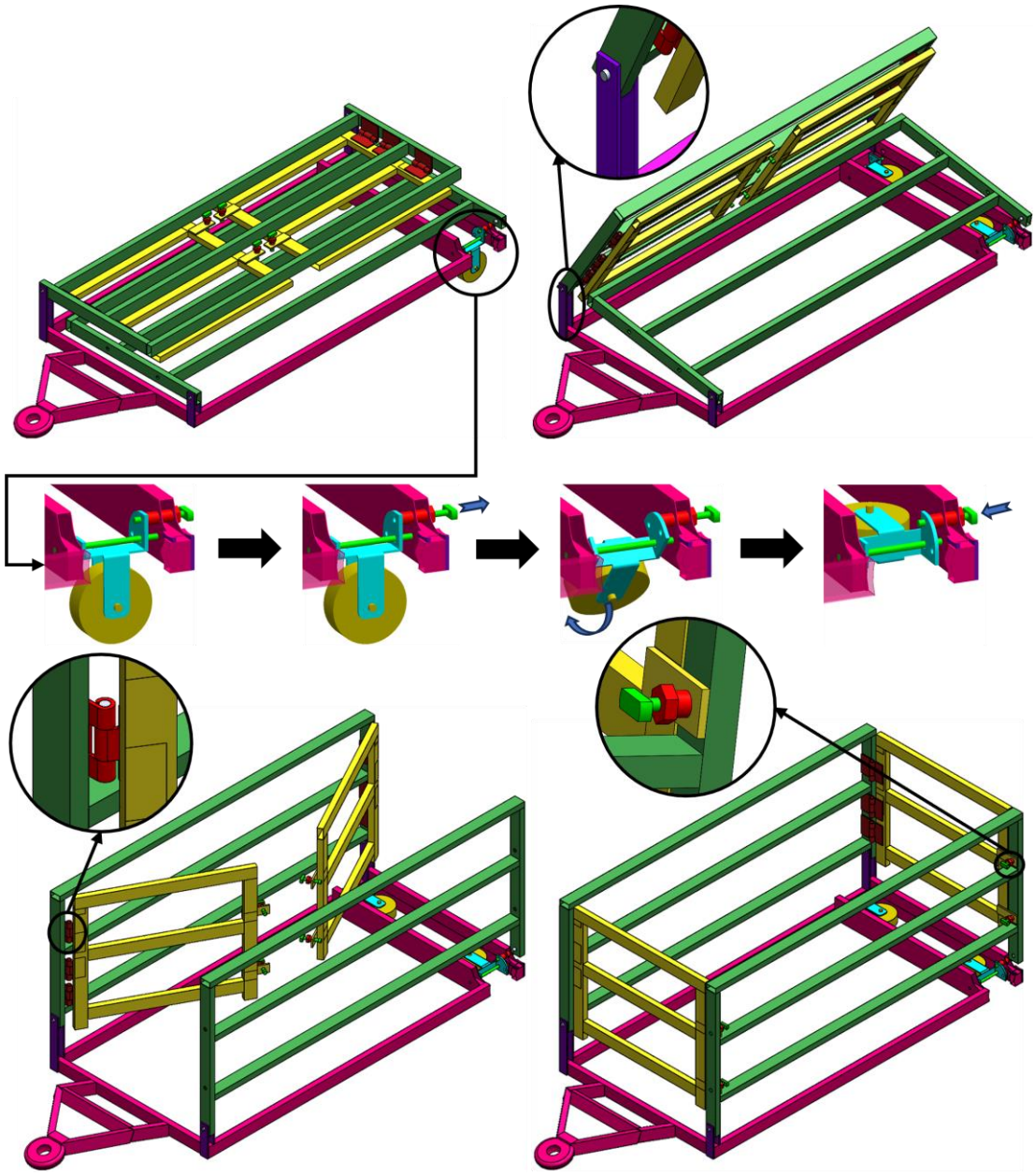

Fig. 15. The process from the transport state into
the working state of the folding frame water tank

The stress and displacement diagrams are shown in Fig. 17. The results show that the position subject to the maximum stress is at the hinge position of the frame assembly and has the value σ_{max} = 146.76 N/mm^2 < [σ] = 163.33 N/mm^2 (according to SS400 Steel with the yield strength S_{yt} = 245 N/mm^2 [17] and the factor of safety (*fs*) is 1.5). The maximum displacement occurs at the center position of the horizontal bar near the bottom of the frame. The maximum displacement value is 1.758 mm, which is an acceptable value. Hence, the folding frame of the water tank ensures strength.

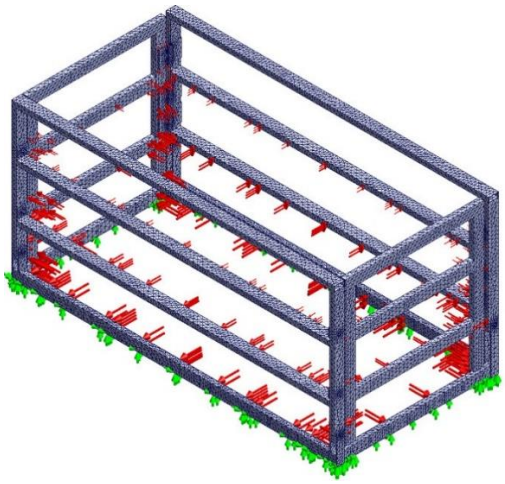

Fig. 16. Mesh and force applied on the folding frame water tank

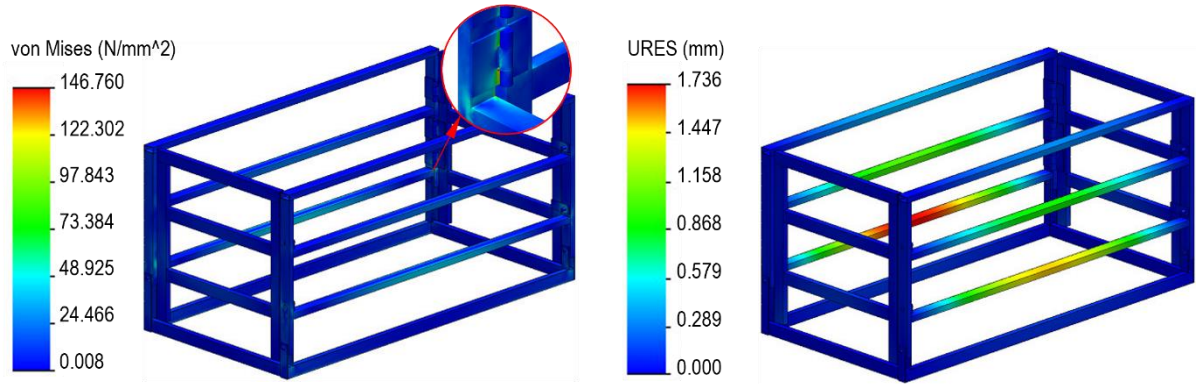

Fig. 17. The results of folding frame simulation (a) Stress distribution diagram, (b) Displacement diagram

6. CONCLUSIONS

In this paper, a compact firefighting vehicle based on the SNAPPER LT14H33 lawn mower is described. In order to add firefighting features, a water sprayer system and a folding frame water tank have been installed on the vehicle chassis. The vehicle has a simple structure and compact size, and is easy to manufacture and maintain at an affordable price. The water sprayer system contains an SCN 30 power sprayer driven by the vehicle's transmission through a belt and a chain drive. The powertrain system is designed to be compact and does not affect the lawn mower blade's drive system. The water sprayer system has the ability to spray water about 13 meters high with a flow rate of 38 L/min. The folding frame tank is made of steel boxes in a rectangular shape that can hold about 500 liters of water. When the vehicle moves, the frame can be folded and connected to the vehicle's rear like a trailer. The vehicle can move in a road space of only 1.3 m and has a maximum speed of about 15 km/h. The proposed compact firefighting vehicle accommodates residential areas within a 1-2 km radius with narrow roads, high population, and house density in least developed and developing countries (e.g., Vietnam,

Laos, Cambodia). Where it's tough to get to the normal fire truck in time. Furthermore, during the daily routine, the vehicle can be utilized for watering plants and applying insecticides on the campus. This paper has added a helpful feature but does not lose the inherent function of the original vehicle, improving the vehicle's value in use.

Acknowledgment

We acknowledge the support of time and facilities from Ho Chi Minh City University of Technology (HCMUT), VNU-HCM for this study.

References

1. Baixia Z. 2017. „Fire Situations and Prevention Measures of residental building". *MATEC Web of Conferences* 100: 00062. ISSN: 2261-236X. DOI: https://doi.org/10.1051/matecconf/201710002062.
2. Sivakumar C., R. Malathy, P. Sivaprakash. 2018. „A Study on Fire Safety on Residental and Commercial Construction Sites". *Archives of Civil Engineering* 64(2): 161-174. ISSN: 1230-2945. DOI: http://doi.org/10.2478/ace-2018-0022.
3. Littlewood J.R., M. Alam, S. Goodhew, G. Davies. 2017. „The 'Safety Gap' in buildings: Perceptions of Welsh Fire Safety Professionals". *Energy Procedia* 134(86): 787-796. ISSN: 1876-6102. DOI: https://doi.org/10.1016/j.egypro.2017.09.586.
4. Reddy P.V.P., M.Y. Reddy. 2021. „Development of Multi-Purpose Agricultural Vehicle by using Solar Power". *International Journal of Engineering Research & Technology* 10(4). ISSN: 2278-0181. DOI: https://doi.org/10.17577/IJERTV10IS040027.
5. Kataboina S.K., M.J. Reddy, K. Dusarlapudi. 2020. „Multi-functional Electrical Vehicle for Agricultural Applications". *Journal of Advanced Research in Dynamical and Control Systems* 12(2): 101-110. ISSN: 1943023X. DOI: http://doi.org/10.5373/JARDCS/V12I2/S202010012.
6. Belyakov V.V., P.O. Beresnev, D.V. Zeziulin, A.A. Kurkin, V.S. Makarov, V.I. Filatov. 2018. „Development of a Multifunctional All-Terrain Vehicle Equipped with Intelligent Wheel-Drive System for Providing Increased Level of Energy Efficiency and Improved Fuel Economy". In: *Proceedings of the Scientific-Practical Conference „Research and Development - 2016"*: 179-188. The Ministry of Education and Science of the Russian Federation. 14-15 December 2016, Moscow, Russia. ISBN: 978-3-319-62869-1.
7. Mahesh S., A. Keshav, A.G. Hegde, M.A. Nair, K.A. Hebbar. 2020. „Electrical Multipurpose Agricultural Vehicle". *International Research Journal of Engineering and Technology* 7(5). ISSN: 2395-0056.
8. USERMANUAL. „Snapper ELT140H331KV Users Manual". Available at: https://usermanual.wiki/Snapper/SnapperElt140H331KvUsersManual225987.835576269/html.
9. TASCO. „SANCHIN SCN 30 POWER SPRAYER". Available at: https://tasco.co.id/product/20-power-sprayers-jet-cleaner/246-sanchin-scn-30-power-sprayer.
10. Bhandari V.B. 2010. *Design of machine elements.* India: Tata McGraw-Hill. ISBN: 978007068179-8.

11. Young D.F., B.R. Munson, T.H. Okiishi, W.W. Huebsch. 2010. *A Brief Introduction to Fluid Mechanics*. United States of America: Wiley. ISBN: 978-0470-59679-1.
12. DIN 2215:1975-03. *Endless V Belts; Dimensions.* Berlin: German Institute for Standardisation Registered Association.
13. Khurmi R.S., J.K. Gupta. 2005. *A Textbook of Machine Design (S.I UNITS).* India: Eurasia Publishing House. ISBN: 978-8121925372.
14. Interlloy. „1045 Medium Tensile Carbon Steel Bar". Available at: http://www.interlloy.com.au/our-products/carbon-steels/1045-medium-tensile-carbonsteelbar/#:~:text=1045%20is%20a%20medium%20tensile,170%20%2D%20210%20in%20either%20condition.
15. ISO/R 733:1969. *Rectangular or square parallel keys and their corresponding keyways (Dimensions in millimeters).* Technical Committee ISO/TC 16.
16. SKF. „UCF 204". Available at: https://www.skf.com/us/products/mounted-bearings/ball-bearing-units/flanged-ball-bearing-units/productid-UCF%20204.
17. JIS F 3101:2015. *Rolled steels for general structure.* Japan: Japanese Standards Association.

Received 29.06.2023; accepted in revised form 01.09.2023